Preparation and characterization of supported bimetallic gold–iron nanoparticles, and its potential for heterogeneous catalysis

Ghaniya Ferouani[1] · Nawal Ameur[1,2] · Redouane Bachir[1]

Abstract

Bimetallic gold–iron catalysts supported on ZrO_2 and TiO_2 were prepared by under potential deposition. The characterization of the catalysts was performed using an inductively coupled plasma, energy-dispersive spectroscopy, diffuse reflectance ultraviolet–visible spectroscopy (DR/UV–vis), and transmission electron microscopy. The catalytic properties of the prepared materials in synthesis of isoxazol-5-(4H)-ones in a one-pot three-component reaction of aromatic aldehydes, ethyl acetoacetate, and hydroxylamine hydrochloride were studied. The chemical structures of the different reaction products were confirmed by ^1H NMR, ^1C NMR. The noteworthy advantages of our simple method, which occurred in efficient, simple, clean, green, mild conditions, and easy workup, gave different isoxazol-5-(4H)-ones with good to high yields (66–78%). The reuse of the catalyst shows that this catalyst can be used up to three cycles without any change in the yield of products.

Keywords Green nanocatalysis · Au–Fe/ZrO_2 · Au–Fe/ZrO_2 · One-pot synthesis · Catalyst reuse

Introduction

Heterocyclic compounds are of great importance to both gold nanoparticles having proved an interesting activity in catalytic reactions; for this reason it has recently become a very attractive subject for many scientists [1, 2]. The birth of the catalysis

---

✉ Ghaniya Ferouani
g-ferouani@live.com

[1] Laboratory of Catalysis and Synthesis in Organic Chemistry, University of Tlemcen, BP 119, Tlemcen, Algeria

[2] High School of Electrical and Energetic Engineering of Oran (ESGEE), Bir El Djir, Algeria

by gold began with a prediction of Geoffrey Bond and Graham Hutching [3] who during the 1970s anticipated that if gold was subdivided into very small particles, it would have very different properties from those in its massive state. At the end of the 1980s, Haruta and al. [4] discovered that gold catalysis is very active in the oxidation reaction of carbon monoxide at low temperature (25–70 °C), a reaction which no other metal was capable to have in such temperature. This marked the birth of the catalysis by gold, which aroused an increasing interest of the scientific and industrial community.

Nano-bimetallic catalysts, which are widely used in many important industrial processes, are often better than their monometallic counterparts in terms of catalytic activity and/or selectivity [5–7]. Bimetallic catalysts supported on metal oxides are of great interest [8, 9] and especially those containing gold proved to be useful in various catalytic applications, i.e., carbon monoxide oxidation [2, 10, 11], hydrogen production [12], and biomass processes [13].

These last two decades have witnessed a great interest in green organic synthesis methods for their ease of use and their respect for the environment and economical manipulations [14–17]. Among these methods, one-pot multi-component reactions (MCRs) with more than two reactants combined in a single-step process have been extensively coveted [11, 12, 18–20]. They are simple workup procedures which allow the synthesis of complex molecules without intermediates isolation. Moreover, the use of heterogeneous catalysts in one-pot multi-component reaction is becoming more and more interesting. Indeed, this has several advantages such as catalyst separation, reusability, long catalytic life, and atom economy and eco-friendly protocols [16, 21–27]. Recently, different pertinent works using heterogeneous catalysts in organic synthesis are realized such as Cu/Al_2O_3, Ag/Bentonite, and CuO/eggshell catalysts used in the reduction in nitro-compounds and organic dyes [28–30], Ag nanoparticles implicated as catalyst for the cyanation of aryl and heteroaryl aldehydes [31], Pd/coral reef in the synthesis of nitriles [32], Pd/MnO_2 used in the one-pot synthesis of tetrazole derivatives [33], and Cu/ZrO_2 for the extraction of 7-hydroxy-4-methoxy-isoflavon from Commelina [34] and others.

In this work and for the first time, we report the synthesis of a novel heterogeneous bimetallic gold $Au–Fe/ZrO_2$ and $Au–Fe/TiO_2$ catalysts made by under potential deposition (UPD). Their potential suitability as catalysts for "green reactions" is proved for the first time, according to our belief, using bimetallic catalysts, catalyzed one-pot multi-component reaction of isoxazol-5-(4H)-ones derivatives under a solvent-free condition at room temperature.

The products we want to synthesize are important five-membered heterocycles characterized by a nitrogen–oxygen bond, useful in various syntheses of other heterocycles such as 1,3-oxazin-6-ones, pyrroles, imidazoles, tetrahydropyridines, pyridopyrimidines, and 2H-azirines [35–38]. The isoxazol-5(4H)-ones derivatives exhibited a growing interest due to their attractive pharmacological properties [39]. They have been broadly used as antibacterial [40], anticonvulsant, antifungal, antidiabetic, anticancer, and hypoglycemic [38, 41–43] and are described as GABA-A receptors and potent inhibitors of PTP1B [44]. The 3,4-disubstituted isoxazole-5(4H)-ones backbone is also a structural component of a variety of natural products and drugs such as ibotenic acid and isoxazole-4 carboxylic acid, [45] which are active agrochemical compounds used
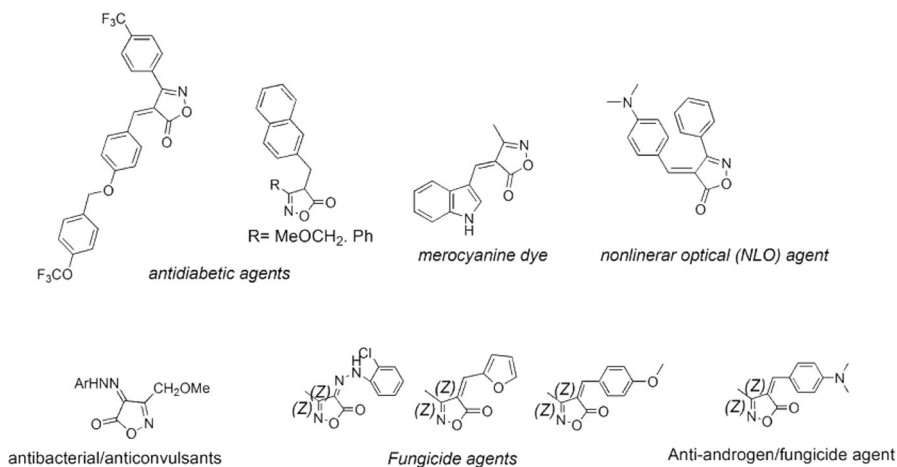
Fig. 1 Interesting isoxazol-5-(4H)-one containing compounds
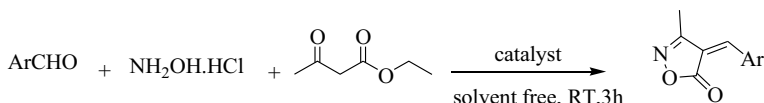
Scheme 1 Synthesis of isoxazol-5(4H)-ones derivatives

as fungicides and insecticides [46], with a wide variety of applications in light-conversion molecular devices, [47] nonlinear optical research, and optical storage and filter dyes in photographic films [48, 49] (see Fig. 1).

There are various methods for the synthesis of substituted isoxazole-5 (4H)-ones [40, 50–52]. For instance, a number of catalysts were used in a three-component condensation of β-oxoesters, hydroxylamine hydrochloride, and aromatic aldehydes, including sodium acetate in aqueous ethanol under visible light [53], pyridine in H_2O under ultrasonic irradiation [54], potassium hydrogen phthalate (KHP) in H_2O at 50 °C [55], and sodium sulfide in ethanol at room temperature [56]. Other methods also used include DABCO in ethanol [57], 2-HSBA [58], boric acid [59], NBS [60], LiBr [40], and sulfated polyborate under a solvent-free condition at 80 °C [46] and which were also reported for the preparation of isoxazole-5(4H)-ones.

We have developed a new rapid and efficient protocol with good and inexpensive green gold nanocatalysis under mild reaction conditions (solvent-free condition at room temperature) (Scheme 1).

Experimental

Catalyst preparation

Catalyst preparation was realized in two steps. The first one concerns the monometallic 1%Au/ZrO$_2$ and 1%Au/TiO$_2$ catalysts prepared by deposition precipitation by urea (DPU) [8]. Briefly, a suspension of support (ZrO$_2$ or TiO$_2$) was introduced into a three-necked flask and heated to 80 °C. Then, a solution of gold salt, HAuCl$_4$·3H$_2$O (10 g L^{-1}), was mixed with urea (0.9 g). All were closed and stirred for 16 h at the same temperature in the dark. At the end, the solid was separated by centrifugation and washed with distilled water many times. The resulting solids were dried at 80 °C overnight (dried catalyst). Finally, the as-prepared catalysts were annealed under H$_2$ gas at 300 °C during 4 h (2 °C min^{-1}).

The second step concerns the iron deposition on the monometallic catalyst by under potential deposition (UPD) [9]. The parent Au/TiO$_2$ or Au/ZrO$_2$ catalysts (0.25 g) was introduced into a glass reactor where it is activated under hydrogen flow at 150 °C (see Fig. 2). Then, a solution (50 mL) of formic acid (pH = 3.7, [Fe^{3+}]=10^{-4} M), previously outgassed under nitrogen flow in the degassing bulb, was introduced onto the catalyst at room temperature under hydrogen flow (200 mL min^{-1}). Finally, the solution of Fe(NO$_3$)$_3$·9H$_2$O dissolved in formic acid and outgassed under nitrogen, was introduced onto the catalyst. After 15 min, the solution was eliminated by filtration and the catalyst was dried under nitrogen flow at 120 °C and then reduced under hydrogen at 150 °C for 2 h 10.

Fig. 2 Montage using for the preparation of bimetallic catalysts
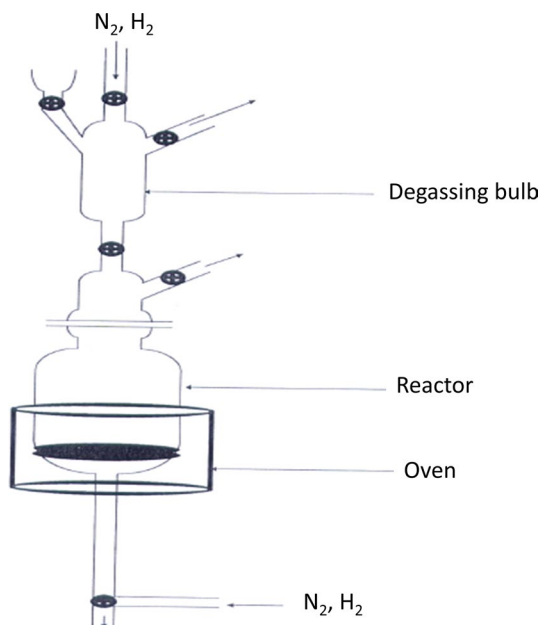
Characterization techniques

The Au effective contents, Fe and Cl in the catalysts, were determined by ICP chemical analysis. TEM micrographs and EDS spectra were obtained from a JOEL JEM-100CXII instrument operating at 120 kV with a resolution of 0.35 nm. DR/UV–vis spectroscopy measurements were taken at room temperature with a Lambda 800 UV–vis spectrometer in the range of 200–800 nm. This setup was equipped with a diffuse reflectance accessory set to collect diffuse reflected light only.

Test catalytic

A mixture of ethyl acetoacetate (10 mmol, 1.30 g), hydroxylamine hydrochloride (10 mmol, 0.69 g), aromatic aldehyde (10 mmol), and (0.04 g 4%) of catalyst was stirred at room temperature. After the completion of the reaction as monitored by TLC, the obtained solid was filtered off and washed with diethyl ether.

Yield and turnover frequency (TOF) were calculated using the following equations:

$$Yield = 100 \times \frac{n_{initial} - n_{final}}{n_{initial}}$$

$$TOF = \frac{n_{initial} - n_{final}}{Time(h) \times Weight\ of\ catalyst\ (g)}$$

Results and discussion

Catalyst characterizations

Figure 3 shows the corresponding spectra of TiO_2, Au/TiO_2, and $Au–Fe/TiO_2$ catalysts. Titania shows the presence of the anatase phase (JCPDS Files No.: 21-1272). The metallization of this support does not show any changes in the resulting spectra. This may be related to the low amount of metals in these materials.

Zirconia-based catalysts show the same results; no peaks related to the metallic species are present (see Fig. 4).

The ICP analysis results of mono- and bimetallic catalysts are shown in Table 1. It is clear that 80–90% of gold in solution were deposited in the supports by deposition precipitation with urea (DPU). However, more than 50% of Fe were deposited on monometallic catalysts using UPD method. Finally, a very low content in Cl in all catalysts was observed. This may be related to the washing of the catalysts and the UPD process.

DR/UV–vis spectrum of ZrO_2 one (see Fig. 5) shows two maxima centered at 224 and 267 nm related to the electronic transition between Zr^{4+} and oxygenated ligand like O_2 or H_2O [8, 61, 62] _ENREF_3. The metalized catalysts show an important band around 540 nm, which is a characteristic resonance plasmon band (SPR) of
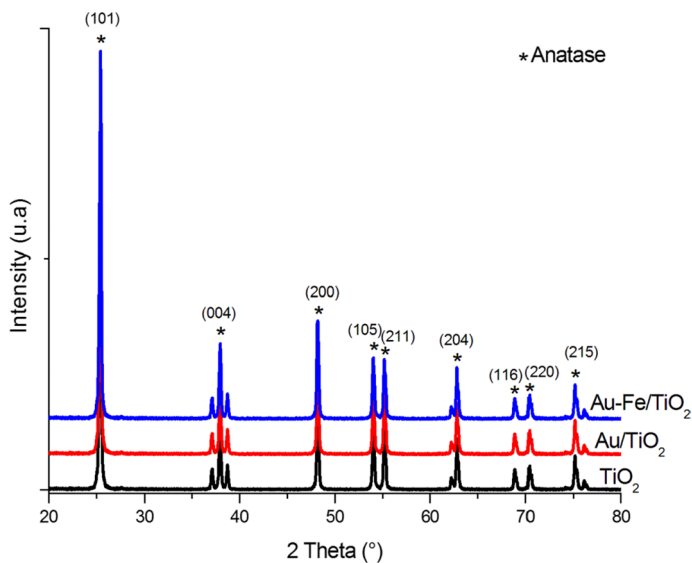
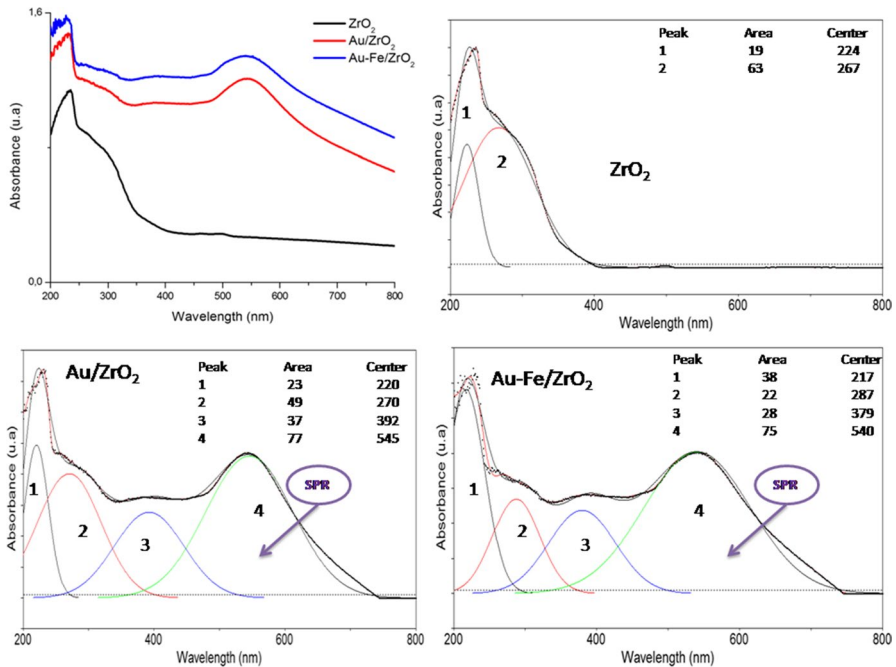**Fig. 3** XRD spectra of doped-TiO$_2$ catalysts
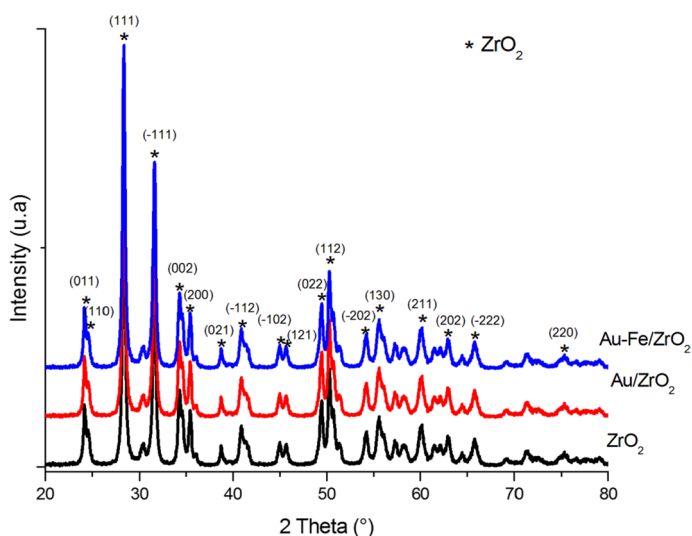
Fig. 4 XRD spectra of doped-ZrO$_2$ catalysts

reduced and spherical gold nanoparticles [8, 63–65]. We may attribute the band in the region 379–392 nm to the gold cluster nanoparticles [66].

The TiO$_2$ deconvolution shows the presence of three bands localized at 207, 269, and 332 nm. The first one might be associated with the ligand–metal charge transfer between tetrahedrical Ti^{4+} and oxygenated ligand such as O–H, O–Ti, or H$_2$O [67],

Table 1 ICP analyses

Catalysts	Au (wt%)	Fe (wt%)	Cl (%)	d (nm)
Au/ZrO$_2$	0.8	–	<0.02	6
Au–Fe/ZrO$_2$	0.75	0.52	<0.0002	5.8
Au/TiO$_2$	0.9	–	<0.02	3.4
Au–Fe/TiO$_2$	0.8	0.92	<0.002	4.3

Fig. 5 RD/UV–vis spectra of doped-ZrO$_2$ catalysts

the second was related to the Ti^{4+} cations in octahedral environment [60, 61], and the last one may be attributed to the anatase phase [8, 67–69]. The resonance plasmon band (SPR) of reduced and spherical gold nanoparticles appears at 549 nm for mono- and bimetallic catalysts. This means that the iron deposition does not affect the gold nanoparticles (see Fig. 6).

Finally, we noticed that the iron species did not show any absorption band which is related to the low amount of this metal (see Table 1).

TEM images of doped-TiO$_2$ catalysts show that gold particles are well distributed on the titania surface (Fig. 7). The deposition of iron does not have important changes in the distribution or the size of the nanoparticles (increase about 1 nm). The analysis of one particle on the surface by EDS shows the presence of peaks related to Au and Fe at the same time confirming the bimetallic character of this catalyst.
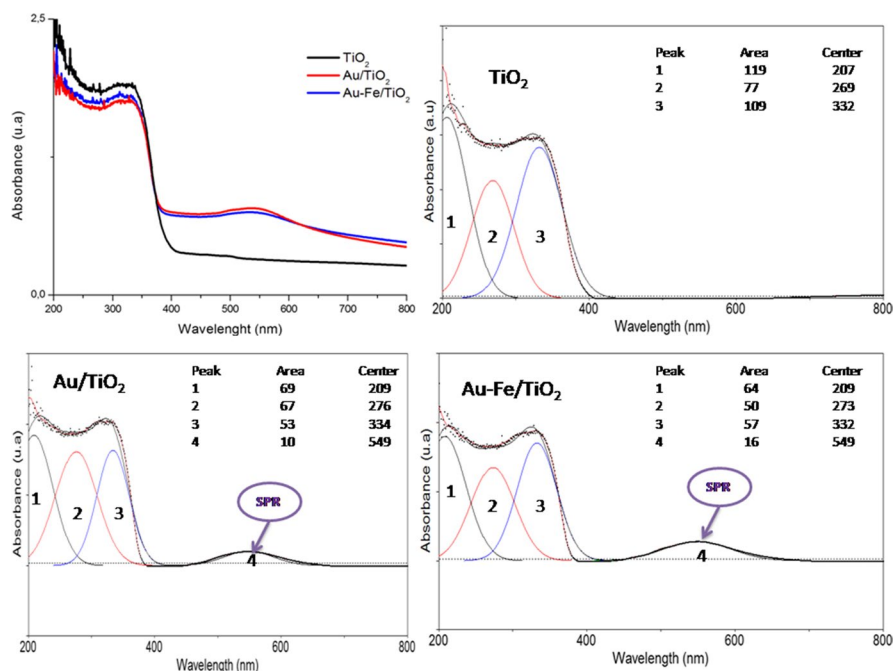
Fig. 6 RD/UV–vis spectra of doped-TiO$_2$ catalysts

Figure 8 shows TEM characterization of Au–Fe/ZrO$_2$. It reveals nano-sized bimetallic Au–Fe particles whose sizes range from 1 to 17 nm with a mean size of 5.7 nm. Moreover, EDS analyses (see Fig. 8) confirm the ICP results and prove the bimetallic character of Au–Fe nanoparticles. In this case, it is clear that Fe deposition (or the acid treatment during Fe deposition) does not affect the size of the metallic species but leads to homogenize the size distribution in comparison with the monometallic catalyst.

By way of conclusion, the preparation of bimetallic catalysts by UPD leads to have a good size distribution of the metallic particles with a bimetallic character. Hence, it is important to evoke the significant role of the support nature. In our previous work, we used the same method to prepare Au–Fe/Al$_2$O$_3$ catalyst [9]. We observed an important agglomeration of the particles with an average size around 37 nm in comparison with the monometallic one with a size around 6 nm. We related this phenomenon to the nature of the support. Alumina is a non-reducible support where the interactions metal-support are weak and the acid treatment induces the facile agglomeration of the particles [9]. In contrast, titania and zirconia are reducible support where the interaction metal-support are strong and the particles show an agglomeration resistance after acid treatment. Finally, the RD/UV–vis results show that the deposition of iron particles does not change the oxidation state of the gold nanoparticles.
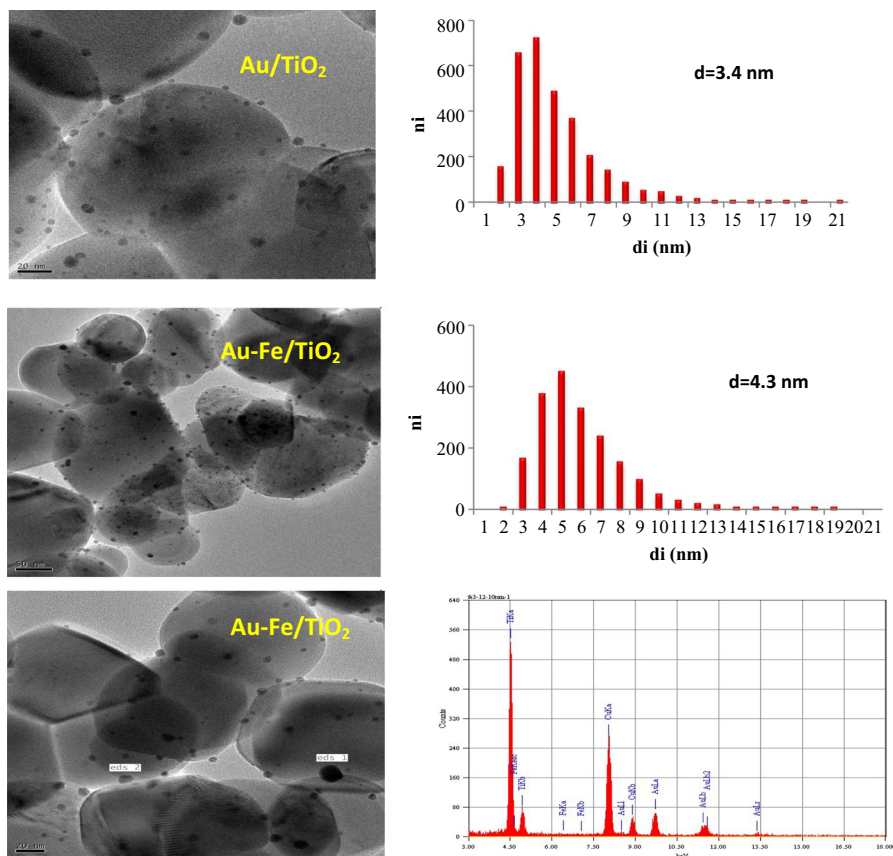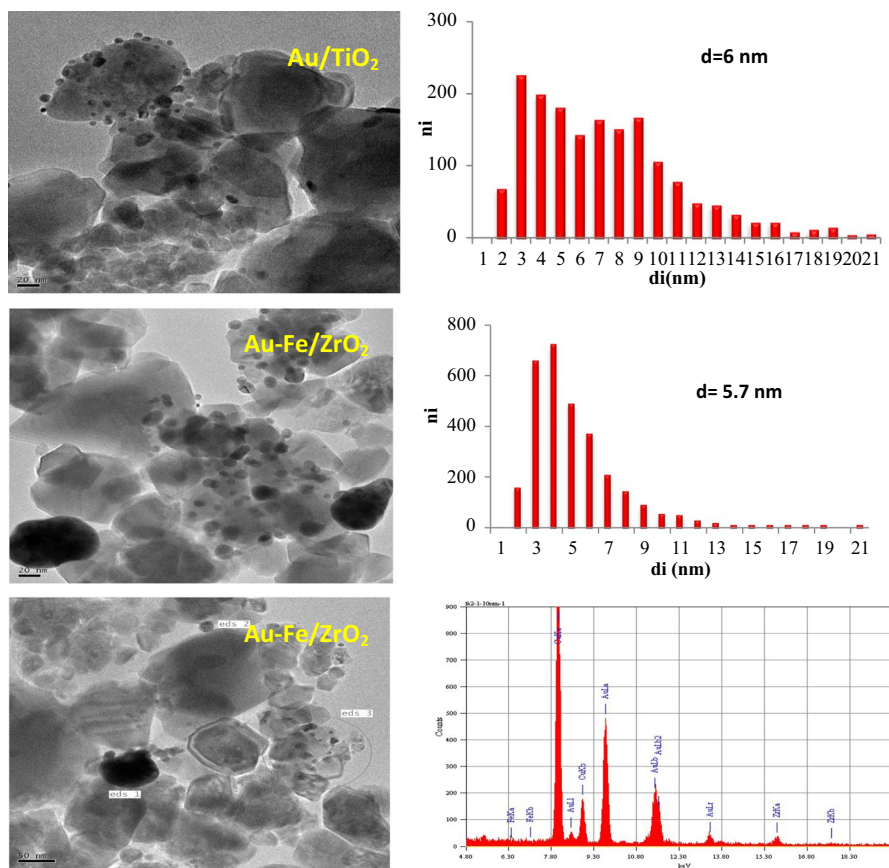
Fig. 7 TEM images, size distributions, and EDS analysis of doped-TiO$_2$ catalysts

Catalytic experiments

The prepared materials were tested for their catalytic activity performance in the synthesis of isoxazol-5-(4H)-ones via a three-component coupling reaction of aromatic aldehydes, ethyl acetoacetate, and hydroxylamine hydrochloride at room temperature. We found that the use of Au–Fe/TiO$_2$ and Au–Fe/ZrO$_2$ as catalysts leads to a yield of 70 and 78% (see Scheme 2), respectively. So, we selected Au–Fe/ZrO$_2$ as the best catalyst to complete the coupling study.

Table 2 shows that the results obtained, the reaction time, and the yield are parameters which strongly depend on the nature of the substituted group on the aromatic aldehyde, and all products were prepared under mild conditions for a relatively short reaction time with high yields. However, we noted that we did not only obtain the products by simple filtration without any purification with a good yield, but we also developed a simpler process, considered as the best for cost and environmental acceptability.

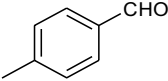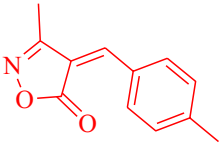**Fig. 8** TEM images, size distribution, and EDS analysis of doped-ZrO$_2$ catalysts
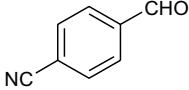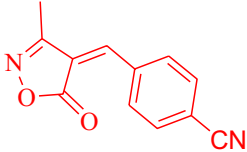

70% using Au-Fe/TiO$_2$ as a catalyst
78% using Au-Fe/ZrO$_2$ as a catalyst
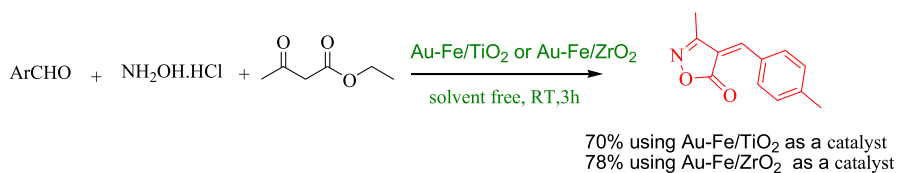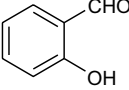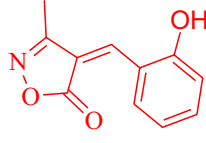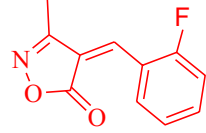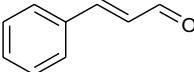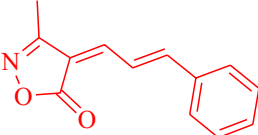
Scheme 2 Influence of the catalyst in the synthesis of Isoxazol-5(4H)-ones derivatives

Mechanism

A tentative mechanism of this reaction is represented in Scheme 3. Oxime inter-mediate C was formed by a 1,2-addition of ethyl acetoacetate and hydroxyl amine in aqueous medium at room temperature, catalyzed by Au–Fe/ZrO$_2$. This catalyst inc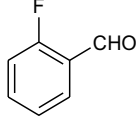reases the carbonyl electrophilicity. During the subsequent Knoevenagel conden-sation, the catalyst promotes the reaction between the activated methylene and the

Table 2 Synthesis of isoxazol-5(4H)-one derivatives **4a–e** uses various aldehydes

Entry	Aldehyde	Product	Yield (%)[a]	TOF (mol.h^{-1}.g^{-1})
1		**4a**	78%	0.0936
2		**4b**	66%	0.0792
3		**4c**	76%	0.0912
4		**4d**	75%	0.0900
5		**4e**	69%	0.0828

[a]Isolated yields

Scheme 3 Suggested mechanism for synthesis of isoxazol-5-(4H)-one derivative

aldehyde. As a result, the alkene intermediate D may form. The final step, an intramolecular O-attack followed by cyclization of the Knoevenagel adduct gives the title compound.

Catalyst stability

The reusability of the catalyst is important for large-scale operations and industrial point of view. Thus, the Au–Fe/ZrO$_2$ recovery and reusability were examined. The catalyst was recovered by a simple filtration, washed with acetone several times, and then dried before use for the next cycle. The reusability of the catalyst was investigated in one-pot reaction of 4-methylbenzaldhyde, ethyl acetoacetate, and hydroxylamine hydrochloride under a solvent-free condition at room temperature. The results reported in Table 3 show that the catalyst can be recovered and reused several times without loss of activity.

Spectroscopic data of some synthesized

(Z)-4-(4-methylbenzylidene)-3-methylisoxazol-5(4H)-one (**4a**), yield: 78%, mp 132–133 °C; 1H NMR (400 MHz, CDCl3): δ_{ppm} 8.21–8.19 (2H, d, *J* = 8.00 Hz,

Table 3 Results of the reaction run in the presence of recycled catalyst	Run	Fields (%)[a]	TOF (mol h^{-1} g^{-1})
	1	78	0.0936
	2	77	0.00924
	3	77	0.00924

[a]Isolated yields

$H_{aromatic}$); 7.3245 (1H, s, CH); 7.25–7.23(2H, d, $J = 8.00$ Hz, $H_{aromatic}$); 2.37 (3H, s, CH_3); 2.21 (3H, s, CH_3) ppm. ^{13}C NMR (400 MHz, CDCl$_3$): δ_{ppm} 168.22; 161.23; 149.98; 145.73; 134.15; 129.95; 129.89; 118.41; 22.06; 11.63 ppm. IR (neat/cm^{-1}): 1730.40; 1698.34; 1169.28.

*(Z)-4-((3-methyl-5-oxoisoxazol-4(5H)-ylidene) methyl) benzonitrile (**4b**)*, Yield: 66%; mp193–194 °C, ^{1}H NMR (400 MHz, DMSO-d$_6$):): δ_{ppm} 8.46–8.44 (2H, d, $J = 8.00$ Hz, $H_{aromatic}$); 8.06–8.04 (3H, t, CH + $H_{aromatic}$); 2.31 (3H, s, CH_3) ppm, ^{13}C NMR (400 MHz, DMSO-d$_6$):): δ_{ppm} 167.73; 162.53; 149.29; 136.56; 133.68; 132.92, 130.34, 122.35, 118.74, 115.09, 11.74 ppm. IR (neat/cm^{-1}): 1720.70; 1675.30; 1055.50; 2265.25.

*(Z)-4-(2-hydroxybenzylidene)-3-methylisoxazol-5(4H)-one (**4c**)*, yield: 76%, mp 203–204 °C; ^{1}H NMR (400 MHz, DMSO-d$_6$): δ_{ppm} 11.00 (1H, s, OH); 8.75–8.73(1H, d, $J = 8.00$ Hz, $H_{aromatic}$); 8.09 (1H, s, CH), 7.47–7.51 (1H, t, $H_{aromatic}$), 7.03–7.00 (1H, d, $J = 12$ Hz, $H_{aromatic}$), 6.95–6.91 (1H, t, $H_{aromatic}$), 2.26 (3H, s, CH_3) ppm, ^{13}C NMR (400 MHz, DMSO-d$_6$): δ_{ppm} 168.73, 162.59, 160.11, 145.45, 137.19, 132.78, 119.95, 119.56, 116.90, 116.60, 11.65 ppm. IR (neat/cm^{-1}): 1770.02; 1670.25; 1080.25.

*(Z)-4-(2-fluorobenzylidene)-3-methylisoxazol-5(4H)-one (**4d**)*, Yield: 75%; mp 159–160 °C; ^{1}H NMR (400 MHz, CDCl$_3$): δ_{ppm} 8.22–8.19 (1H, d, $J = 8.00$ Hz, $H_{aromatic}$); 7.92–7.90 (1H, d, $J = 12$ Hz, $H_{aromatic}$); 7.45–7.39 (1H, m, $H_{aromatic}$); 7.32 (1H, s, CH); 7.24–7.19 (1H, m, $H_{aromatic}$); 2.24 (3H, s, CH_3) ppm. ^{13}C NMR (400 MHz, CDCl$_3$): δ_{ppm} 167.50; 163.76; 161.30; 160.91; 148.11 (d, $J = 12$ Hz); 134.00 (d, $J = 32$ Hz); 130.54 (d, $J = 32$); 129.87 (d, $J = 12$ Hz); 121.02 (d, $J = 84$ Hz); 119.72 (d, $J = 92$ Hz); 11.59 ppm. IR (neat/cm^{-1}): 1731.15; 1640.98.

*(Z)-3-methyl-4-((E)-3-phenylallylidene)isoxazol-5(4H)-one (**4e**)*, Yield: 69%; mp 172–173 °C; ^{1}H NMR (400 MHz, CDCl$_3$): δ_{ppm} 8.35–8.28 (dd, $J = 12$ Hz, 1H, CH), 7.66–7.64 (2H, m, CH=CH), 7.44–7.43 (3H, m, $H_{aromatic}$),; 7.32–8.26 (2H, m, $H_{aromatic}$); 2.25 (s, 3H, CH_3)ppm ^{13}C NMR (400 MHz, CDCl$_3$): δ_{ppm} 168.94; 159.78; 151.31; 147.45; 135.00; 131.53; 129.18; 128.93; 122.47; 117.99; 11.15 ppm. IR (neat/cm^{-1}): 1735.00; 1670.21.

Conclusion

We described the synthesis of a bimetallic gold Au–Fe/TiO$_2$ and Au–Fe/ZrO$_2$ catalysts produced by under potential deposition, which has been used as an efficient catalyst for the preparation of heterocyclic compounds (3-methyl-4-arylmethylene-isoxazol-5(4H)-ones) in high yields involving one-pot operations and short reaction times. The new heterogeneous catalyst is simple, highly efficient, and recyclable in this protocol. This environmentally friendly process has many advantages, namely solvent-free condition, small quantities of waste, ease of product isolation, efficiency, low cost, and mild and green conditions.

References

1. D. Wang, A. Villa, F. Porta, L. Prati, D. Su, J. Phys. Chem. C **112**, 23 (2008)
2. T. Murayama, M. Haruta, Chin. J. Catal. **37**, 10 (2016)
3. G. Bond, P. Sermon, Gold Bull. **6**, 4 (1973)
4. M. Haruta, T. Kobayashi, H. Sano, N. Yamada, Chem. Lett. **16**, 2 (1987)
5. F. Boccuzzi, E. Guglielminotti, F. Pinna, G. Strukul, Surf. Sci. **377**, 728 (1997)
6. Y. Wang, Z. Xiao, L. Wu, Curr. Org. Chem. **17**, 12 (2013)
7. H. Goksu, H. Sert, B. Kilbas, F. Sen, Curr. Org. Chem. **21**, 9 (2017)
8. N. Ameur, S. Bedrane, R. Bachir, A. Choukchou-Braham, J. Mol. Catal. A Chem. **374–375**, 1 (2013)
9. N. Ameur, A. Berrichi, S. Bedrane, R. Bachir, Adv. Mater. Res. **856**, 48 (2014)
10. A. Venezia, L. Liotta, G. Pantaleo, V. La Parola, G. Deganello, A. Beck, Z. Koppány, K. Frey, D. Horvath, L. Guczi, Appl. Catal. A **251**, 2 (2003)
11. X. Liu, A. Wang, L. Li, T. Zhang, C.-Y. Mou, J.-F. Lee, J. Catal. **278**, 2 (2011)
12. L. Rong, H. Han, H. Jiang, Y. Dai, M. Zhuang, M. Cao, S. Tu, J. Heterocycl. Chem. **46**, 5 (2009)
13. S. Albonetti, T. Pasini, A. Lolli, M. Blosi, M. Piccinini, N. Dimitratos, J.A. Lopez-Sanchez, D.J. Morgan, A.F. Carley, G.J. Hutchings, Catal. Today **195**, 1 (2012)
14. P. Anastas, N. Eghbali, Chem. Soc. Rev. **39**, 1 (2010)
15. G. Brahmachari, B. Banerjee, Current. Green Chem. **2**, 3 (2015)
16. S.F.F. Hamzavi, S. Jamili, M. Yousefzadi, A.M. Moradi, N.A. Biuki, Bull. Chim. React. Eng. Catal. **14**, 1 (2019)
17. B.A. Dar, S.W. Safvi, M.A. Rizvi, Bull. Chim. React. Eng. Catal. **13**, 1 (2018)
18. Y.M. Litvinov, V.Y. Mortikov, A.M. Shestopalov, J. Comb. Chem. **10**, 5 (2008)
19. Essid, S. Touil, Curr. Org. Chem. **14**, 2 (2017)
20. K. Alali, F. Lebsir, S. Amri, A. Rahmouni, E. Srasra, N. Besbes, Bull. Chim. React. Eng. Catal. **14**, 1 (2019)
21. S.N. Maddila, S. Maddila, W.E. van Zyl, S.B. Jonnalagadda, RSC Adv. **5**, 47 (2015)
22. R. Pagadala, S. Maddila, S. Rana, S.B. Jonnalagadda, RSC Adv. **4**, 13 (2014)
23. H. Naeimi, A. Didar, J. Mol. Struct. **1137**, 626 (2017)
24. A. Berrichi, R. Bachir, M. Benabdallah, N. Choukchou-Braham, Tetrahedron Lett. **56**, 11 (2015)
25. A. Berrichi, R. Bachir, S. Bedrane, N. Choukchou-Braham, K. Belkacemi, Res. Chem. Intermed. **45**, 6 (2019)
26. O. Zimou, B. Malek, A. Elhallaoui, T. Ghailane, R. Ghailane, S. Boukhris, N. Habbadi, A. Hassikou, A. Souizi, Bull. Chim. React. Eng. Catal. **14**, 2 (2019)
27. R.D. Kusumaningtyas, I.N. Aji, H. Hadiyanto, A. Budiman, Bull. Chim. React. Eng. Catal. **11**, 1 (2016)
28. M. Nasrollahzadeh, Z. Issaabadi, S.M. Sajadi, Compos. Part B Eng. **166**, 112 (2019)
29. S.M. Sajadi, K. Kolo, S.M. Hamad, S.A. Mahmud, A.A. Barzinjy, S.M. Hussein, ChemistrySelect **3**, 12274 (2018)
30. S.M. Sajadi, K. Kolo, S.M. Abdullah, S.M. Hamad, H.S. Khalid, A.T. Yasin, Surf. Interfaces **13**, 205 (2018)
31. S.M. Sajadi, M. Nasrollahzadeh, R. Akbari, ChemistrySelect **4**, 1127 (2019)
32. M. Nasrollahzadeh, F. Ghorbannezhad, S.M. Sajadi, R.S. Varma, Nanomaterials **9**, 565 (2019)
33. M. Nasrollahzadeh, F. Ghorbannezhad, S.M. Sajadi, Appl. Organometal Chem. **33**, 4698 (2019)
34. S.M. Hamad, S.A. Mahmud, S.M. Sajadi, Z.A. Omar, Surf. Interfaces **15**, 125 (2019)
35. G. Abbiati, E.M. Beccalli, G. Broggini, C. Zoni, Tetrahedron Lett. **59**, 50 (2003)
36. S. Tu, J. Zhang, R. Jia, B. Jiang, Y. Zhang, H. Jiang, Org. Biomol. Chem. **5**, 9 (2007)
37. K. Okamoto, T. Shimbayashi, M. Yoshida, A. Nanya, K. Ohe, Angew. Chem. Int. Ed. **55**, 25 (2016)
38. F. Risitano, G. Grassi, F. Foti, R. Romeo, Synthesis **2002**, 01 (2002)
39. B. Kafle, N.G. Aher, D. Khadka, H. Park, H. Cho, Chem. Asian J. **6**, 8 (2011)
40. G. Ferouani, A. Nacer, N. Ameur, R. Bachir, C. Ziani-Cherif, J. Chin. Chem. Soc. **65**, 4 (2018)
41. M.S. Chande, R.S. Verma, P.A. Barve, R.R. Khanwelkar, R. Vaidya, K. Ajaikumar, Eur. J. Med. Chem. **40**, 11 (2005)
42. M. Aaglawe, S.S. Dhule, S.S. Bahekar, P.S. Wakte, D.B. Shinde, J. Korean Chem. Soc. **47**, 2 (2003)
43. M. Gordaliza, G.T. Faircloth, M.A. Castro, J.M.M. del Corral, M.L. López-Vázquez, A.S. Feliciano, J. Med. Chem. **39**, 14 (1996)

44. B. Frolund, U. Kristiansen, L. Brehm, A.B. Hansen, P. Krogsgaard-Larsen, E. Falch, J. Med. Chem. **38**, 17 (1995)
45. C.H. Stammer, A.N. Wilson, C.F. Spencer, F.W. Bachelor, F.W. Holly, K. Folkers, J. Am. Chem. Soc. **79**, 12 (1957)
46. M.S. Patil, C. Mudaliar, G.U. Chaturbhuj, Tetrahedron Lett. **58**, 33 (2017)
47. S. Biju, M. Reddy, R.O. Freire, Inorg. Chem. Commun. **10**, 4 (2007)
48. E. Aret, H. Meekes, E. Vlieg, G. Deroover, Dye. Pigments **72**, 3 (2007)
49. X.-H. Zhang, Y.-H. Zhan, D. Chen, F. Wang, L.-Y. Wang, Dye Pigments **93**, 1 (2012)
50. R. Laroum, A. Debache, Synth. Commun. **48**, 14 (2018)
51. J.J. Donleavy, E.E. Gilbert, J. Am. Chem. Soc. **59**, 6 (1937)
52. D.B. Lowe, S. Magnuson, N. Qi, A.-M. Campbell, J. Cook, Z. Hong, M. Wang, M. Rodriguez, F. Achebe, H. Kluender, Bioorg. Med. Chem. Lett. **14**, 12 (2004)
53. F. Saikh, J. Das, S. Ghosh, Tetrahedron Lett. **54**, 35 (2013)
54. K. Ablajan, H. Xiamuxi, Synth. Commun. **42**, 8 (2012)
55. H. Kiyani, F. Ghorbani, Res. Chem. Intermed. **41**, 10 (2015)
56. Q. Liu, X. Hou, Phosphorus Sulfur Silicon Relat Elem **187**, 4 (2012)
57. M. Mirzazadeh, G.H. Mahdavinia, J. Chem. **9**, 1 (2012)
58. H. Kiyani, H. Darbandi, A. Mosallanezhad, F. Ghorbani, Res. Chem. Intermed. **41**, 10 (2015)
59. H. Kiyani, F. Ghorbani, Res. Chem. Intermed. **41**, 5 (2015)
60. H. Kiyani, A. Kanaani, D. Ajloo, F. Ghorbani, M. Vakili, Res. Chem. Intermed. **41**, 10 (2015)
61. F. Boccuzzi, G. Cerrato, F. Pinna, G. Strukul, J. Phys. Chem B **102**, 30 (1998)
62. D. Prasetyoko, Z. Ramli, S. Endud, H. Nur, J. Mol. Catal A Chem **241**, 1 (2005)
63. P. Mulvaney, Langmuir **12**, 3 (1996)
64. S. Johnson, S. Evans, S. Mahon, A. Ulman, Langmuir **13**, 1 (1997)
65. R. Grisel, P. Kooyman, B. Nieuwenhuys, J. Cell. Biochem. **191**, 2 (2000)
66. A. Simakov, I. Tuzovskaya, N. Bogdanchikova, A. Pestryakov, M. Avalos, M.H. Farias, E. Smolentseva, Catal. Commun. **9**, 6 (2008)
67. M. Cozzolino, M. Di Serio, R. Tesser, E. Santacesaria, Appl. Catal. A **325**, 2 (2007)
68. E.A. Cloutis, K.A. McCormack, J.F. Bell, A.R. Hendrix, D.T. Bailey, M.A. Craig, S.A. Mertzman, M.S. Robinson, M.A. Riner, Icarus **197**, 1 (2008)
69. N. Ameur, R. Bachir, S. Bedrane, A. Choukchou-Braham, J. Chin. Chem. Soc. **64**, 9 (2017)